PROCEEDINGS OF THE ROYAL SOCIETY A

FirstCite® e-publishing

Proc. R. Soc. A
doi:10.1098/rspa.2008.0094
Published online

Tristability of thin orthotropic shells with uniform initial curvature

By S. Vidoli[1,*] and C. Maurini[2,3]

[1]*Dipartimento di Ingegneria Strutturale e Geotecnica, Università di Roma La Sapienza, via Eudossiana 18, 00184 Rome, Italy*
[2]*UPMC Univ. Paris 06, and* [3]*CNRS, UMR 7190, Institut Jean Le Rond d'Alembert, F-75005 Paris, France*

Composite shells show a rich multistable behaviour of interest for the design of shape-changing (morphing) structures. Previous studies have investigated how the initial shape determines the shell stability properties. For uniform initial curvatures and orthotropic material behaviour, not more than two stable equilibria have been reported. In this paper, we prove that untwisted, uniformly curved, thin orthotropic shells can have up to three stable equilibrium configurations. Cases of tristability are first documented using a numerical stability analysis of an extensible shallow shell model. Including mid-plane extension shows that the shells must be sufficiently curved in relation to their thickness to be multistable. Thus, an inextensible model allows us to perform an analytical stability analysis. Focusing on untwisted initial configurations, we illustrate with simple analytical results how the material parameters of the shell control the dependence of its multistable behaviour on the initial curvatures. In particular, we show that when the bending stiffness matrix approaches a degeneracy condition, the shell exhibits three stable equilibria for a wide range of initial curvatures.

Keywords: morphing structures; multistability; bistable shells; Gaussian curvature; shape control

1. Introduction

Multistability and geometrical nonlinear effects are of interest for the design of structures with embedded actuation and shape control applications. In suitably designed structures, a limited actuation force may lead to a major change in shape by triggering instability phenomena, or simply by exploiting displacement amplifications due to geometrical nonlinearities. Moreover, multistable structures may hold several equilibrium configurations without the need for continued actuation. In nature, a beautiful and inspiring example of the efficiency of multistability in compensating for the lack of a powerful muscle-like action is the Venus flytrap. This plant captures its prey by triggering the snapping of its

* Author for correspondence (stefano.vidoli@uniroma1.it).

Electronic supplementary material is available at http://dx.doi.org/10.1098/rspa.2008.0094 or via http://journals.royalsociety.org.

Received 4 March 2008
Accepted 20 May 2008

leaves, which behave like multistable shells (Forterre *et al.* 2005). Current research seeks to adopt similar ideas in engineering structures by exploiting the geometrical nonlinear effects typical of thin shells and the actuation capabilities offered by the latest generation of piezoelectric materials and shape memory alloys. Similar properties reveal their importance in a multitude of engineering applications encompassing deployable structures, shape-changing mirrors for active focusing in adaptive optical systems, mechanical memory cells, valves, micropumps, variable geometry engine exhausts and reconfigurable aeroplane wings with embedded actuation (morphing wings).

Several numerical and experimental studies (Hyer 1981; Schultz *et al.* 2006; Bowen *et al.* 2007; Portela *et al.* 2008) have analysed the bistability of multilayered composite plates with unsymmetric stacking sequences and investigated the possibility of using a single surface-bonded piezoelectric macro-fibre composite actuator to allow the plates to snap between the two equilibria. To model this system, Hyer and Schultz (Hyer 1981; Schultz *et al.* 2006) used a Rayleigh–Ritz approach based on von Kármán plate kinematics; Mattioni *et al.* (2007) and Portela *et al.* (2008) used shell models with linear constitutive behaviour but including geometrical nonlinearities to compare experimental results with the simulations obtained by a finite-element commercial code. Those studies are limited to the numerical and/or experimental analysis of specific structures, showing a reasonable agreement among experimental results, numerical computations and semi-analytical approaches. Guest & Pellegrino (2006) and Seffen (2007) provided a deeper insight into the phenomenon of multistability of shallow shells by recalling the crucial role of geometry and the interplay between extension and curvature (e.g. Love 1906; Mansfield 1989). With simplified uniform curvature models, they approached the difficult problem of studying the influence of geometry and material properties on multistability. Considering that the deformations of thin shells are almost inextensible, Guest & Pellegrino (2006) used an inextensible model to analyse the bistability of composite cylindrical shells (i.e. shells with zero Gaussian curvature). Seffen (2007) adopted an extensible uniform curvature model to investigate the range of initial curvatures for which orthotropic shells are bistable. He showed that even isotropic shells may be bistable, but in numerical investigations he was unable to find more than two stable equilibria. To the best of our knowledge, the recent contribution of Norman *et al.* (2008) is the first to show a case of tristability. This is obtained for a special corrugated shallow shell through a coupling between the corrugation curvature and the curvature at the macro scale.

This paper extends the approaches and the results of Guest & Pellegrino (2006) and Seffen (2007) to show that orthotropic shallow shells with uniform initial curvature may be tristable and discusses the range of initial curvatures and material parameters leading to tristability. Section 2 presents the basic equations of the shell model in the framework of the uniform curvature assumption used by Forterre *et al.* (2005), Guest & Pellegrino (2006) and Seffen (2007). Focusing on the role played by the shell extensibility and the Gaussian curvature, it discusses both the extensible and inextensible variants and comments on the respective conditions of applicability. Section 3 revisits the case study of the orthotropic shallow shell analysed by Seffen (2007) and shows that there are combinations of initial curvatures and material parameters for

which the shell becomes tristable. Section 4 repeats the stability analysis using an inextensible shell model and focusing on untwisted configurations. With this simplified approach, the regions of the initial curvature space for which the shell is tristable are given analytically as a function of the material parameters of the shell. This information provides criteria for enhancing the range of initial curvatures leading to tristability. Section 5 concludes the paper.

2. Uniform curvature models

(*a*) *Extensible model*

Within Kirchhoff–Love theory (e.g. Love 1906 or Podio Guidugli 1991), deformations of thin shells are specified by two 2×2 symmetric tensor fields defined on the shell mid-surface, the surface extension $\boldsymbol{\epsilon}$ and the surface curvature $\boldsymbol{\kappa}$. Using Voigt notation, these tensors are represented by the following lists:

$$\boldsymbol{\epsilon} = \{\epsilon_x, \epsilon_y, 2\epsilon_{xy}\} \quad \text{and} \quad \boldsymbol{\kappa} = \{\kappa_x, \kappa_y, 2\kappa_{xy}\}, \tag{2.1}$$

where (x, y) are the reference coordinates of the mid-plane points.

Let $\boldsymbol{\kappa}_0$ be the shell initial curvature, i.e. the curvature in a stress-free reference configuration. The change of curvature with respect to this initial shape is denoted by $\boldsymbol{\Delta\kappa} = \boldsymbol{\kappa} - \boldsymbol{\kappa}_0$; the initial extension is assumed to vanish and $\boldsymbol{\Delta\epsilon} = \boldsymbol{\epsilon}$. The shell extension and the change of curvature are not independent. *Gauss's celebrated Theorema Egregium* of the theory of curved surfaces states that the Gaussian curvature,

$$g := \det \boldsymbol{\kappa} = \kappa_x\kappa_y - \kappa_{xy}^2, \tag{2.2}$$

is invariant under local isometries of the surface. The inextensibility of the shell thus translates into the condition $g = g_0$, where $g_0 := \det \boldsymbol{\kappa}_0$ is the initial Gaussian curvature. For small membranal deformations of shallow shells (e.g. Calladine 1983; Mansfield 1989), the variation of the Gaussian curvature and the in-plane extensions are related by the following compatibility equation:

$$-\Delta g = \frac{\partial^2 \epsilon_y}{\partial x^2} + \frac{\partial^2 \epsilon_x}{\partial y^2} - 2\frac{\partial^2 \epsilon_{xy}}{\partial x\, \partial y}, \tag{2.3}$$

where $\Delta g := g - g_0$ denotes the variation of the Gaussian curvature with respect to the initial value. Seffen (2007), revisiting Mansfield (1962), derived a simplified model by assuming that the curvature tensor is constant. Here, we closely follow this approach by assuming that the curvatures $\boldsymbol{\kappa}$ and $\boldsymbol{\kappa}_0$ are uniform throughout the shell. To maintain the parallel with Seffen (2007), only orthotropic homogeneous shells are considered. Thus, for a linear constitutive behaviour, the elastic energy of the shell is written as the sum of the contributions due to bending (first term) and stretching (second term),

$$\mathcal{U}(\boldsymbol{\epsilon}, \boldsymbol{\kappa}) = \frac{1}{2} S\bar{\boldsymbol{D}}\boldsymbol{\Delta\kappa}\cdot\boldsymbol{\Delta\kappa} + \frac{1}{2}\int_{\mathcal{S}} \bar{\boldsymbol{A}}\boldsymbol{\epsilon}\cdot\boldsymbol{\epsilon}\, \mathrm{d}x\, \mathrm{d}y, \tag{2.4}$$

where $\mathcal{S}$ is the shell mid-surface and S is its area. The constitutive matrices $\bar{\boldsymbol{A}}$ and $\bar{\boldsymbol{D}}$ are the extensional and bending stiffnesses, respectively. For homogeneous

orthotropic shells of thickness t, they are in the form

$$\bar{\boldsymbol{D}} = \frac{t^3 E_0}{12}\begin{bmatrix} 1 & \nu & 0 \\ \nu & \beta & 0 \\ 0 & 0 & \rho\left(1-\dfrac{\nu^2}{\beta}\right) \end{bmatrix} \quad \text{and} \quad \bar{\boldsymbol{A}} = tE_0\begin{bmatrix} 1 & \nu & 0 \\ \nu & \beta & 0 \\ 0 & 0 & \rho\left(1-\dfrac{\nu^2}{\beta}\right) \end{bmatrix}. \tag{2.5}$$

Here, $\beta := E_y/E_x$ is the ratio of the Young's moduli in the coordinate directions; ν is the Poisson ratio; ρ is the dimensionless shear modulus; and $E_0 = E_x/\left(1-\nu^2/\beta\right)$ is a scaling constant. The matrices $\bar{\boldsymbol{D}}$ and $\bar{\boldsymbol{A}}$ must be positive definite. Using the Sylvester criterion of positive definiteness,[1] this condition translates into the following requirements on β, ν and ρ:

$$\beta > \nu^2 \quad \text{and} \quad \rho > 0. \tag{2.6}$$

Without loss of generality, we further assume that $\nu^2 < \beta \leq 1$; this assumption is equivalent to naming the axes in such a way that $E_x \geq E_y$. The energy in equation (2.4) does not include the term due to coupling between extension and bending, which is found in the unsymmetric composite plates considered by Hyer (1981).

In the distribution of the in-plane strains, $\boldsymbol{\epsilon}$ may be obtained by rewriting the compatibility equation (2.3) in terms of the Airy stress function for the in-plane problem. With the uniform curvature hypothesis, the source term Δg appearing in this equation will be constant. Hence, the solution for the in-plane stresses and strains can vary in position but will always remain linear with respect to Δg. Introducing this solution in the extensional contribution to the elastic energy of the shell (2.4) and calculating the integral leads to the following expression of the shell elastic energy in terms of curvatures only:

$$U(\boldsymbol{K}) = \frac{1}{2}\boldsymbol{D}(\boldsymbol{K}-\boldsymbol{H})\cdot(\boldsymbol{K}-\boldsymbol{H}) + \frac{\phi^2}{2}(\det \boldsymbol{K} - \det \boldsymbol{H})^2, \tag{2.7}$$

where

$$\boldsymbol{D} = \frac{12}{E_0 t^3}\bar{\boldsymbol{D}}, \quad U = \frac{12R^2}{E_0 t^3 S}\mathcal{U}, \quad \boldsymbol{K} = R\,\boldsymbol{\kappa} \quad \text{and} \quad \boldsymbol{H} = R\,\boldsymbol{\kappa}_0, \tag{2.8}$$

where R is the characteristic radius of curvature of the shell. The non-dimensional constant ϕ characterizes the relative energy penalty of stretching and bending deformations.

This may be written in the form

$$\phi = \frac{S^*}{Rt}, \tag{2.9}$$

where S^* is an equivalent shell mid-plane surface depending on the material properties and the geometry of the shell planform. For a shell with an elliptical planform and homogeneous boundary conditions, Seffen (2007) provided the analytical solution of the in-plane stresses and strains as a function Δg and

[1] A matrix is positive definite if and only if all of the leading principal minors are positive.

calculated the exact value of ϕ, which corresponds to

$$S^* = S\sqrt{\frac{1-\nu^2/\beta}{6\pi^2(1/r^2 + r^2/\beta + 1/3(1/\rho - 2\nu/\beta))}}. \tag{2.10}$$

The geometric parameter $r := b/a$ is the ratio between the semi-axes of the ellipse, supposed to be oriented along the directions of material symmetry. For shells with more complex shapes, the general reasoning and the expression (2.9) for ϕ are still valid, but the equivalent surface S^* must be obtained with a numerical solution of the in-plane problem (2.3). The boundary conditions are satisfied exactly only for special geometries, such as a shell with elliptic planform and lenticular cross section (Mansfield 1962; Seffen 2007). The uniform curvature assumption otherwise neglects the influence of the boundary conditions on the bending moment and of the associated boundary-layer effects.

(*b*) *Inextensible limit*

For large values of the parameter ϕ, the energy functional (2.7) penalizes the difference between the initial Gaussian curvature $G_0 := \det \boldsymbol{H}$ and the actual Gaussian curvature $G := \det \boldsymbol{K}$. Owing to Gauss's Theorema Egregium, this difference is related to the extensional deformation of the shell mid-plane. In the inextensible model obtained in the limit $\phi \to \infty$, the curvature tensor $\boldsymbol{K}$ must lie in the constant Gaussian curvature manifold,

$$\mathcal{G}(\boldsymbol{H}) := \{\boldsymbol{K} \in \mathrm{Sym}, \det \boldsymbol{K} = \det \boldsymbol{H}\}, \tag{2.11}$$

where Sym is the vector space of symmetric second-order 2×2 tensors, isomorphic to $\mathbb{R}^3$. The stable equilibria of the inextensible model are the constrained minima of the bending energy,

$$U_b(\boldsymbol{K}) := \frac{1}{2}\boldsymbol{D}(\boldsymbol{K}-\boldsymbol{H})\cdot(\boldsymbol{K}-\boldsymbol{H}), \tag{2.12}$$

under the inextensibility constraint $\det \boldsymbol{K} = \det \boldsymbol{H}$. The sign of the initial Gaussian curvature G_0 deeply influences the behaviour of the shell and calls for a special classification: cylindrical (or parabolic) shells for $G_0 = 0$; cup-like (or elliptic) shells for $G_0 > 0$; and saddle-like (or hyperbolic) shells for $G_0 < 0$.

The inextensible model is justified for $\phi^2 \gg 1$, i.e. for $R^2 t^2 \ll S^{*2}$. This means that the shell must be thin and sufficiently curved,[2] so that

$$\frac{1}{R^2} \gg \left(\frac{t}{S^*}\right)^2. \tag{2.13}$$

Also for very thin shells, the extensibility must be accounted for if the curvatures are small, i.e. such that $R \sim S^*/t$.

[2] For a specific shell with given initial curvature $\boldsymbol{\kappa}_0$, $1/R$ should be intended as the order of magnitude of $\boldsymbol{\kappa}_0$, for instance $1/R = \|\boldsymbol{\kappa}_0\|$. In our analysis, the initial curvature will be left as a free parameter; thus, the choice of R is arbitrary and is equivalent to a rescaling of the dimensionless curvatures (see also point (iii) of §3*b*). If R is chosen according to (2.13), i.e. such that $\phi \gg 1$, then the shell is almost inextensible for non-dimensional curvatures $\boldsymbol{H}$ of the order of 1.

3. Stable equilibria of the extensible model

(a) Equilibrium and stability

The equilibria of the extensible model are the points of stationarity of (2.7), i.e. the solutions of

$$\frac{\partial U}{\partial \boldsymbol{K}} = \boldsymbol{D}(\boldsymbol{K}-\boldsymbol{H}) + \phi^2(\det \boldsymbol{K} - \det \boldsymbol{H})\boldsymbol{K}^A = \boldsymbol{0}, \tag{3.1}$$

where $\boldsymbol{K}^A := \partial(\det \boldsymbol{K})/\partial \boldsymbol{K} = \{K_y, K_x, -K_{xy}\}$ is the gradient of the Gaussian curvature. Equation (3.1) is a coupled system of third-order polynomial equations in the three unknown components of $\boldsymbol{K}$, which may have several real solutions, say $\boldsymbol{K}_{1,2,\ldots}(\boldsymbol{H})$. Physically, only stable equilibria are of interest. A sufficient condition for stability of the equilibrium $\boldsymbol{K}_i$ is the positive definiteness of the Hessian matrix,

$$\boldsymbol{M}_i(\boldsymbol{H}) := \left.\frac{\partial^2 U}{\partial \boldsymbol{K}^2}\right|_{\boldsymbol{K}_i} = [\boldsymbol{D} + \phi^2 \boldsymbol{K}^A \otimes \boldsymbol{K}^A + \phi^2(\det \boldsymbol{K} - \det \boldsymbol{H})\boldsymbol{L}]_{\boldsymbol{K}_i}, \tag{3.2}$$

where $\boldsymbol{u}\otimes\boldsymbol{v}$ means the standard tensor product of two vectors $\boldsymbol{u}$ and $\boldsymbol{v}$ and

$$\boldsymbol{L} := \frac{\partial^2 \det \boldsymbol{K}}{\partial \boldsymbol{K}^2} = \begin{bmatrix} 0 & 1 & 0 \\ 1 & 0 & 0 \\ 0 & 0 & -1/2 \end{bmatrix} \tag{3.3}$$

is the constant matrix given by the second gradient of the Gaussian curvature.

It is not feasible to obtain analytical solutions from the equilibrium equation (3.1) for general orthotropic material properties and initial curvatures. Seffen (2007) gave explicit expressions for the equilibria and their stability properties in some peculiar cases, such as isotropic or direct stress isotropic material behaviour and specific initial curvatures. Here, after discussing some general properties of the problem, we explore the solution of this system as a function of the initial curvature by numerical and graphical methods, showing some relevant new results.

(b) General properties

From the analysis of the structure of (2.7), (3.1) and (3.2), one can infer the following general properties of the shell model.

(i) The matrix $\boldsymbol{D}$ is always positive definite and $\boldsymbol{K}^A \otimes \boldsymbol{K}^A$ is positive semi-definite, having a single non-vanishing eigenvalue $\|\boldsymbol{K}^A\|^2$ along the direction of $\boldsymbol{K}^A$. Thus, the sum of the first two contributions to the Hessian matrix (3.2) is always positive definite. The third contribution, $\boldsymbol{L}$, is not definite, having 1, -1 and $-1/2$ as eigenvalues. Moreover, its coefficient, the change in the Gaussian curvature, may be negative. Thus, only this latter term may render an equilibrium unstable.

(ii) The initial state $\boldsymbol{K}=\boldsymbol{H}$ satisfies (3.1) and has a null coefficient on the last term of the Hessian matrix (3.2). Thus, it is always a stable equilibrium. It is also the unique global minimum of (2.7), which is always positive except for $\boldsymbol{K}=\boldsymbol{H}$, where the energy attains its lower bound, zero. In the following, this equilibrium will be denoted by $\boldsymbol{K}_1$ and referred to as *natural* equilibrium.

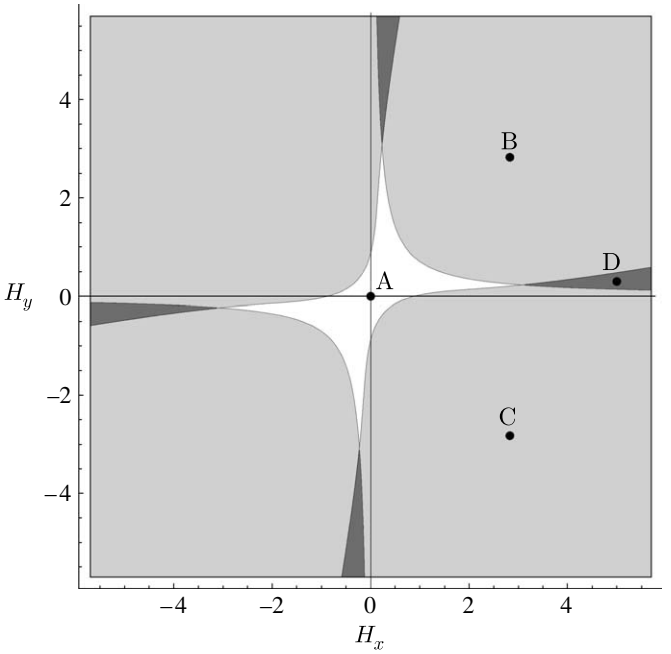

Figure 1. Phase diagram of the extensible model as a function of the initial curvatures for $H_{xy}=0$. The material parameters are $\beta=0.977$, $\nu=0.766$ and $\rho=1.965$, as in Seffen (2007). Dark grey, tristability regions; light grey, bistability regions; white, monostability region.

(iii) The change of ϕ is tantamount to a rescaling of the initial curvature. Indeed, amplifying the norm of the initial curvature $\boldsymbol{H}$ by a constant α ($\boldsymbol{H}\rightarrow\alpha\boldsymbol{H}$) is equivalent to a corresponding change in the scaling radius of curvature ($R\rightarrow R/\alpha$), which, in turn, implies an amplification by α of ϕ ($\phi\rightarrow\alpha\phi$). Thus, in a non-dimensional analysis where the norm of the initial curvature is left free to vary, ϕ is a redundant parameter and may be fixed arbitrarily. This also means that the ratio of stretching-to-bending energies increases with the norm of $\boldsymbol{H}$. For small initial curvatures, the effect of in-plane extension is important, while it may be neglected for large initial curvatures.

(*c*) *Numerical solutions and tristability regions*

Equation (3.1) is a polynomial system. This fact turns out to be very useful in the numerical analysis because modern software programs for algebraic computations include efficient algorithms to find *all* the equilibrium solutions of polynomial equations. Thus, for assigned material properties, it is possible to track all the equilibria as functions of the initial curvature and assess their stability by checking the sign of the eigenvalues of the Hessian matrix (3.2). A stable equilibrium is a real root of (3.1), for which all the three eigenvalues of (3.2) are positive.

Figure 1 reports the number of stable equilibria as a function of the initial curvature in the plane $H_{xy}=0$ (untwisted configurations) for the same set of material parameters used by Seffen (2007) and $\phi=10$. As noted above, the value

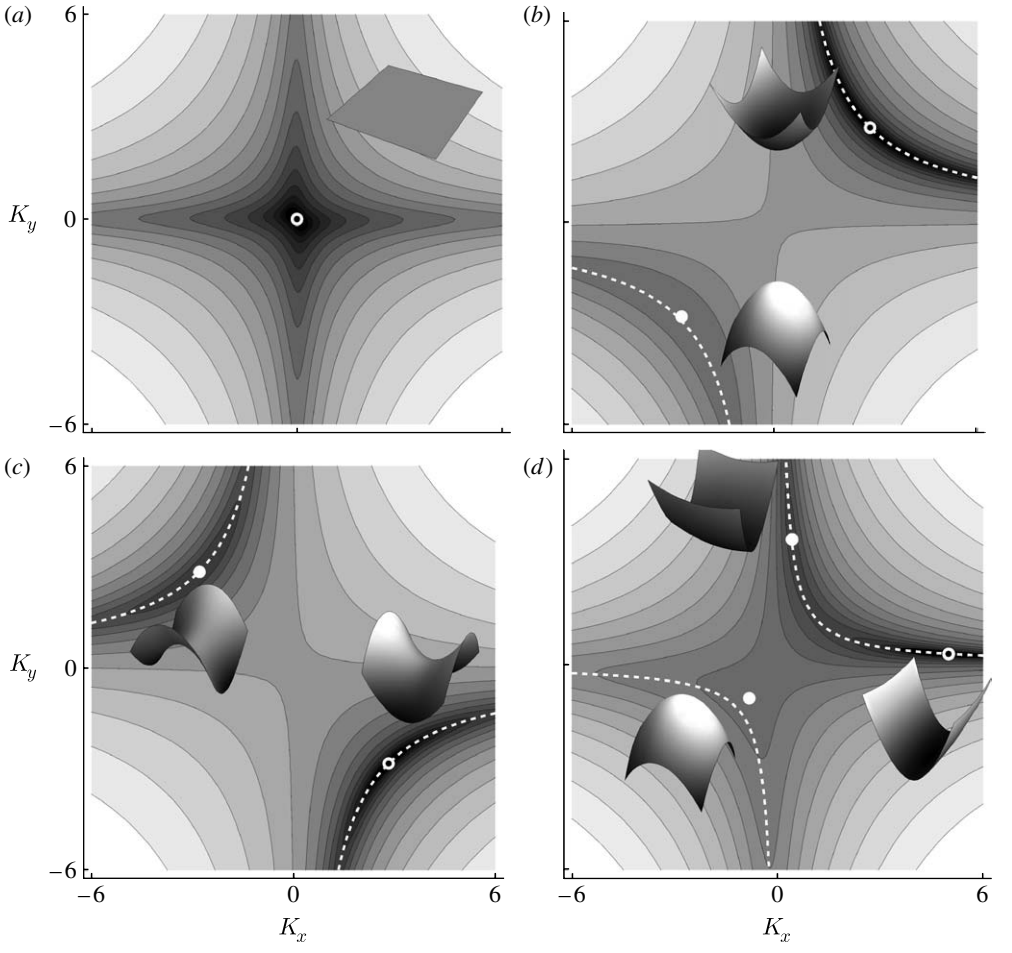

Figure 2. Energy and equilibria of the extensible model for the four initial curvatures ((*a*) A, (*b*) B, (*c*) C and (*d*) D) marked in figure 1. The white points denote the minima, the white–black point denotes the natural configuration and the initial curvature. Sketches of the associated shell shapes are superposed. The dashed white line denotes the sets where det $\boldsymbol{K}=\det \boldsymbol{H}$.

of ϕ may be fixed arbitrarily and is equivalent to a rescaling of $\boldsymbol{H}$. In this phase diagram, shells with initial curvature $\boldsymbol{H}$ inside the white central region have a single stable equilibrium configuration, which is the natural state $\boldsymbol{K}_1=\boldsymbol{H}$. For initial curvatures in the light shaded regions, there are two stable equilibria. The dark shaded regions mark initial states for which the shell is tristable. These regions are not present in the results of Seffen (2007), where the numerical investigation stops at smaller values of the initial curvature, or, equivalently, at smaller ϕ (decreasing ϕ means zooming-in on figure 1). The points A, B, C and D mark initial curvatures leading to four qualitatively different behaviours corresponding to (A) a monostable initially flat shell, (B) a bistable cup-like shell, (C) a bistable saddle-like shell and (D) a tristable shell. Figure 2 reports the contour plots of the associated energy functions (2.7). Each contour plot is represented in the K_x–K_y plane, because, for the assumed orthotropic material behaviour, the equilibria for $H_{xy}=0$ are always with $K_{xy}=0$. However,

computations are completed without this hypothesis and stability along the K_{xy}-direction is checked explicitly.[3] Interestingly, of the three stable equilibria obtained at the point D, two are at similar energy levels and lie in the same 'energy valley'. The regions of tristability appear as tiny slices of the initial curvature plane, and may be difficult to observe experimentally for the present choice of material parameters. The white dashed lines in the plots of figure 2 mark the sets of points verifying the inextensibility condition $G = G_0$; under the hypotheses made, these points lie over the hyperbolae $K_x K_y = G_0 = H_x H_y$. The distance between each of the equilibria and these sets is small, meaning that the shell has an almost inextensible behaviour.

4. Stable equilibria of the inextensible model

Section 3*c* shows that orthotropic shells may be tristable. But the study was limited to specific numerical values of the constitutive parameters. In this section, by adopting the inextensible model described in §2*b*, we investigate how material properties affect the multistability. To obtain analytical results, we will focus on the study of untwisted configurations.

(*a*) *Curvature representation and inextensibility*

As for every symmetric tensor, the shell curvature may be written in terms of its eigenvalues, say k_{I} and k_{II}, and its two mutually orthogonal eigenvectors, say $\boldsymbol{m}(\theta) = \{\cos\theta, \sin\theta\}$ and $\boldsymbol{n}(\theta) = \{-\sin\theta, \cos\theta\}$. The angle θ specifies the orientation of the eigenvectors with respect to the material axes of the orthotropic shell. This corresponds to the following spectral representation of the curvature tensor:

$$\tilde{\boldsymbol{K}}(k_{\mathrm{I}}, k_{\mathrm{II}}, \theta) = k_{\mathrm{I}}\boldsymbol{m}(\theta)\otimes\boldsymbol{m}(\theta) + k_{\mathrm{II}}\boldsymbol{n}(\theta)\otimes\boldsymbol{n}(\theta), \quad \theta \in [0, \pi). \tag{4.1}$$

With this representation, $\det \boldsymbol{K} = k_{\mathrm{I}}k_{\mathrm{II}}$, and the constant Gaussian curvature condition reads as $k_{\mathrm{I}}k_{\mathrm{II}} = G_0$. Hence, all the curvatures respecting the inextensibility constraint (2.11) are written in the form

$$\hat{\boldsymbol{K}}(c, \theta) \coloneqq \tilde{\boldsymbol{K}}(c, G_0/c, \theta) = \begin{bmatrix} c - \dfrac{1}{2}(1 - G_0/c^2)(1 - \cos 2\theta) \\ G_0/c + \dfrac{1}{2}(1 - G_0/c^2)(1 - \cos 2\theta) \\ (1 - G_0/c^2)\sin(2\theta) \end{bmatrix}, \tag{4.2}$$

where $c \in (-\infty, 0) \cup (0, +\infty)$ is one of the principal curvatures and $\theta \in [0, \pi)$. This expression for the curvature of inextensible shells reduces to the coordinate system used by Kebadze *et al.* (2004) and Guest & Pellegrino (2006) for the special case of cylindrical shells, for which $G_0 = 0$. For $c^2 = G_0$, the two principal curvatures are equal, the shell is spherical and the curvature becomes independent of θ.

[3] As shown by Seffen (2007), the equilibria with $K_{xy} = 0$ are stable with respect to twist if the torsional rigidity of the shell, here proportional to ρ, is sufficiently high with respect to the change of the Gaussian curvature: $2(1-\nu^2)\rho/\beta > \phi^2 \Delta G$. This point is discussed further in §4.

The (c, θ) coordinates represent a system of curvilinear coordinates for the constant Gaussian curvature surface $\mathcal{G}(\boldsymbol{H})$. Thus, by defining the energy function $\hat{U}$ in terms of these coordinates,

$$\hat{U}(c,\theta) = U_b(\hat{\boldsymbol{K}}(c,\theta)), \tag{4.3}$$

the equilibria of the inextensible shell model are found as the solutions of

$$\left.\begin{aligned} \frac{\partial \hat{U}}{\partial c} &= \frac{\partial U_b}{\partial \hat{\boldsymbol{K}}} \cdot \frac{\partial \hat{\boldsymbol{K}}}{\partial c} = 0 \\ \text{and} \qquad & \\ \frac{\partial \hat{U}}{\partial \theta} &= \frac{\partial U_b}{\partial \hat{\boldsymbol{K}}} \cdot \frac{\partial \hat{\boldsymbol{K}}}{\partial \theta} = 0. \end{aligned}\right\} \tag{4.4}$$

The stable equilibria are the minima of $\hat{U}(c,\theta)$, with a sufficient minimality condition being the positive definiteness of the Hessian matrix,

$$\hat{M} = \begin{bmatrix} \dfrac{\partial^2 \hat{U}}{\partial c^2} & \dfrac{\partial^2 \hat{U}}{\partial c\, \partial \theta} \\ \dfrac{\partial^2 \hat{U}}{\partial c\, \partial \theta} & \dfrac{\partial^2 \hat{U}}{\partial \theta^2} \end{bmatrix}. \tag{4.5}$$

The full expressions for the energy and its derivatives are easily obtained analytically, but they are too long to be reported here.

(*b*) *Untwisted configurations*

We look for stable untwisted equilibria of shells with an untwisted initial state. These configurations are characterized by $H_{xy}=0$ and $\theta=0$. They automatically satisfy the second equilibrium condition (4.4). The remaining equilibrium equation reads

$$\left.\frac{\partial \hat{U}}{\partial c}\right|_{\theta=0} = \frac{(c-H_x)\big(c^3 - \nu(c+H_x)H_y c + \beta H_x H_y^2\big)}{c^3} = 0. \tag{4.6}$$

The corresponding components of the Hessian matrix are calculated to be

$$\left.\frac{\partial^2 \hat{U}}{\partial c^2}\right|_{\theta=0} = \frac{c^4 + 3\beta H_x^2 H_y^2 - 2cH_xH_y(H_x\beta + H_y\nu)}{c}, \tag{4.7}$$

$$\left.\frac{\partial^2 \hat{U}}{\partial \theta^2}\right|_{\theta=0} = \frac{2(c^2 - H_xH_y)^2}{c^2}\left(\frac{(c-H_x)(c(\nu-1)+(\nu-\beta)H_y)}{(c^2-H_xH_y)} + 2\rho\left(1-\frac{\nu^2}{\beta}\right)\right), \tag{4.8}$$

$$\left.\frac{\partial^2 \hat{U}}{\partial c\, \partial \theta}\right|_{\theta=0} = 0. \tag{4.9}$$

Because the second cross derivative of the energy is equal to zero, the stability of the untwisted equilibria may be checked in the c and θ directions separately. In the following, the stability properties are studied as a function of the initial curvature. To this end, it will be useful to adopt a polar description by defining the norm H, the angle φ and its tangent η, such that

$$\{H_x, H_y\} = H\{\cos\varphi, \sin\varphi\} \quad \text{and} \quad \eta = \tan\varphi. \tag{4.10}$$

(i) *Equilibria and stability along the c-coordinate*

For $\theta = 0$, the shell energy simplifies to

$$\hat{U}(c,0) = \frac{(c - H_x)^2\left(c^2 - 2\nu H_y c + \beta H_y^2\right)}{2c^2}. \tag{4.11}$$

This function is continuous for each $c \neq 0$,

$$\lim_{c\to\pm\infty} \hat{U}(c,0) = +\infty \quad \text{and} \quad \lim_{c\to\pm 0} \hat{U}(c,0) = +\infty. \tag{4.12}$$

Hence, by continuity arguments, $\hat{U}(c,0)$ has at least one minimum for c positive and one minimum for c negative. One of these is always the natural equilibrium $c = H_x$, which solves the equilibrium equation (4.6). Moreover, at $c = H_x$, the second derivative of the energy with respect to c reads

$$\left.\frac{\partial^2 \hat{U}}{\partial c^2}\right|_{\substack{c=H_x \\ \theta=0}} = H_x^4(1 - 2\eta\beta\nu + \beta\eta^2), \tag{4.13}$$

which is positive for each $\beta > \nu^2$ and $H_x \neq 0$. Thus, the natural equilibrium $c = H_x$ is always stable with respect to c. The remaining equilibria are the real roots of

$$c^3 - \nu H_y c^2 + \nu H_x H_y c + \beta H_x H_y^2 = 0. \tag{4.14}$$

Depending on the sign of its discriminant,

$$\Delta = \eta^3 H_x^6(4\beta\eta^2\nu^3 + 4\nu^3 + \eta(\nu^4 + 18\beta\nu^2 - 27\beta^2)), \tag{4.15}$$

the cubic equation (4.14) may have either one real root and a pair of complex conjugate roots ($\Delta < 0$), or three real roots ($\Delta > 0$). In the first scenario, the unique real root must be the second minimum of $\hat{U}(c,0)$ and have a sign opposite to the sign of H_x. In the second case, using continuity arguments, the three roots of (4.14) must be two minima and one maximum. In summary, when θ is blocked to 0, i.e. the twist is constrained, the shell is either bistable or tristable with respect to c. From the solution of the equation $\Delta = 0$, the critical values of η for the passage between bistable and tristable behaviour are found to be $\eta_1^c = 0$ and

$$\eta_{2,3}^c = \frac{\beta}{8\nu^3}\left(27 - \frac{\nu^2}{\beta}\left(18 - \frac{\nu^2}{\beta}\right) \pm \sqrt{\left(1 - \frac{\nu^2}{\beta}\right)\left(9 - \frac{\nu^2}{\beta}\right)^3}\right). \tag{4.16}$$

The roots $\eta_{2,3}^c$ are real for each feasible combination of material constants (2.6) and they have the same sign as the Poisson ratio ν. The system is tristable in c when $\Delta > 0$, i.e. for

$$0 < \eta < \eta_2^c \quad \text{and} \quad \eta > \eta_3^c, \tag{4.17}$$

if $\nu > 0$, or for

$$\eta_3^c < \eta < 0 \quad \text{and} \quad \eta < \eta_2^c, \tag{4.18}$$

if $\nu < 0$, where root naming is such that $\eta_2^c \leq \eta_3^c$.

(ii) *Stability along the θ-coordinate*

The natural equilibrium $c = H_x$ is always stable also with respect to θ,

$$\left.\frac{\partial^2 \hat{U}}{\partial \theta^2}\right|_{\substack{c=H_x \\ \theta=0}} = 4(H_x - H_y)^2(1-\beta/\nu^2)\rho, \tag{4.19}$$

and is always positive except for $H_x = H_y = c$; in this case, the shell is spherical and θ-stability is not meaningful. Equation (4.8) shows that any non-spherical equilibrium will be stable with respect to θ, provided the shear stiffness ρ is sufficiently high to render $\partial^2 \hat{U}/\partial \theta^2 > 0$. However, if ρ is not large enough, equilibria different from the natural equilibrium may lose stability when the configuration c and the initial curvature $(H_x, H_y = \eta H_x)$ satisfy the following singularity conditions:

$$\left.\frac{\partial \hat{U}}{\partial c}\right|_{\theta=0} = 0 \quad \text{and} \quad \left.\frac{\partial^2 \hat{U}}{\partial \theta^2}\right|_{\theta=0} = 0. \tag{4.20}$$

The system (4.20) is fulfilled when the polynomials given by the numerators of equations (4.6) and (4.8) have common roots in c, i.e. when their polynomial resultant[4] with respect to c vanishes,

$$8\eta^5\beta(\beta-\nu^2)^2(\eta(\beta-\nu)^2-(\nu-1)^2)^2 p(\eta) = 0, \tag{4.21}$$

where

$$p(\eta) = (\beta - 2\nu\rho)(1+\beta\eta^2) + \big(4(1-\nu^2/\beta)^2\rho^3 + 8\nu(1-\nu^2/\beta)\rho^2 + (5\nu^2-3\beta)\rho - \beta\nu\big)\eta. \tag{4.22}$$

The two roots of (4.21) obtained for $\eta = (\nu-1)^2/(\beta-\nu)^2$ are not physically meaningful because they correspond to a null θ-stability margin of the equilibria $c = (\nu-1)/(\beta-\nu)$, for which the shell is spherical and θ-stability is not relevant. The remaining solutions of (4.21) are $\eta_1^\theta = 0$ and the two roots of the quadratic polynomial (4.22), say $\eta_{2,3}^\theta$. The latter roots are real if

$$\rho \geq \rho^* = \frac{\sqrt{\beta}}{1+\nu/\sqrt{\beta}}. \tag{4.23}$$

The values of $\eta_{1,2,3}^\theta$ effectively correspond to a change in stability of some equilibria with respect to θ. Hence, we may conclude that, depending on the value of the shear stiffness ρ, there are either one or three critical values of η associated with a change of stability in θ, namely:

[4] Two polynomials have common roots if and only if their polynomial resultant, defined as the product of the differences of their roots, vanishes. Modern algebraic computation software, such as MATHEMATICA, provide efficient algorithms to calculate the polynomial resultant.

— for $\rho<\rho^*$, there is a single change of stability in θ, which is for $\eta=\eta_1^\theta=0$ and
— for $\rho\geq\rho^*$, there are two additional changes of stability for $\eta=\eta_{2,3}^\theta$, roots of (4.22).

(iii) *Tristability regions*

The analysis above shows that, in the inextensible model, the stability properties of untwisted configurations are independent of the norm of the initial curvature H. Equilibria may lose stability only as a result of a change in the initial curvature ratio $\eta=H_y/H_x$. The lines $H_y=\eta_{1,2,3}^{c,\theta}H_x$ partition the H_x–H_y plane in sectors corresponding to initial curvature regions for which the shells have the same number of stable equilibria. An interesting case is obtained when the changes of stability in c and θ occur simultaneously. This happens when the discriminant Δ in equation (4.15) and the polynomial in equation (4.22) have common roots, i.e. when their polynomial resultant vanishes,

$$\beta^7(\beta-\nu^2)^2(3\beta-4\nu\rho)^4(\beta-2\nu\rho)^3(-2\rho\nu^3+\beta(\nu+2\rho)\nu+3\beta^2)^2=0. \tag{4.24}$$

The unique physically admissible root of equation (4.24) with respect to ρ is either

$$\rho_t^+=\frac{3\beta}{4\nu}, \tag{4.25}$$

if $\nu>0$, or

$$\rho_t^-=-\frac{\beta}{2\nu}\frac{(3-\nu^2/\beta)}{(1-\nu^2/\beta)}, \tag{4.26}$$

if $\nu<0$.

Figure 3 reports as a function of ρ and $\varphi:=\tan^{-1}\eta$ the number of stable equilibria obtained with assigned values of β and ν. These plots underline the relevance of the threshold values ρ^* and $\rho_t^\pm$ for the shear stiffness. For a positive Poisson ratio $\nu>0$, figure 3*a* shows the following properties.

— For $\rho<\rho^*$, the negative Gaussian curvature shells ($-\pi/2<\varphi<0$) are monostable, while positive Gaussian curvature shells ($0<\varphi<\pi/2$) are bistable.
— For $\rho^*<\rho<\rho_t^+$, some equilibria gain the stability with respect to θ; the negative Gaussian curvature shells become bistable and the positive Gaussian curvature shells are either bistable or tristable. The limits of the tristability regions are $\varphi_{2,3}^\theta=\tan^{-1}(\eta_{2,3}^\theta)$, with $\eta_{2,3}^\theta$ being the roots of (4.22); across these curves there is a change of stability with respect to twist of one equilibrium.
— For $\rho>\rho_t^+$, the shear stiffness is large enough to secure the twisting stability of all the equilibria and the stability properties no longer depend on ρ. The limits of the tristability regions are $\varphi_{2,3}^c=\tan^{-1}(\eta_{2,3}^c)$, with $\eta_{2,3}^c$ given by equation (4.17). When leaving the tristability region by crossing these lines, two minima and one maximum of $\hat{U}(c,0)$ coalesce into a single minimum. In the terminology of catastrophe theory, this is a cusp catastrophe in c.

For $\nu<0$, figure 3*b* shows a different scenario. In this case, tristability is possible only for negative Gaussian curvature shells; however, the threshold values ρ^* and ρ_t^- for the shear stiffness are numerically much larger than for $\nu>0$.

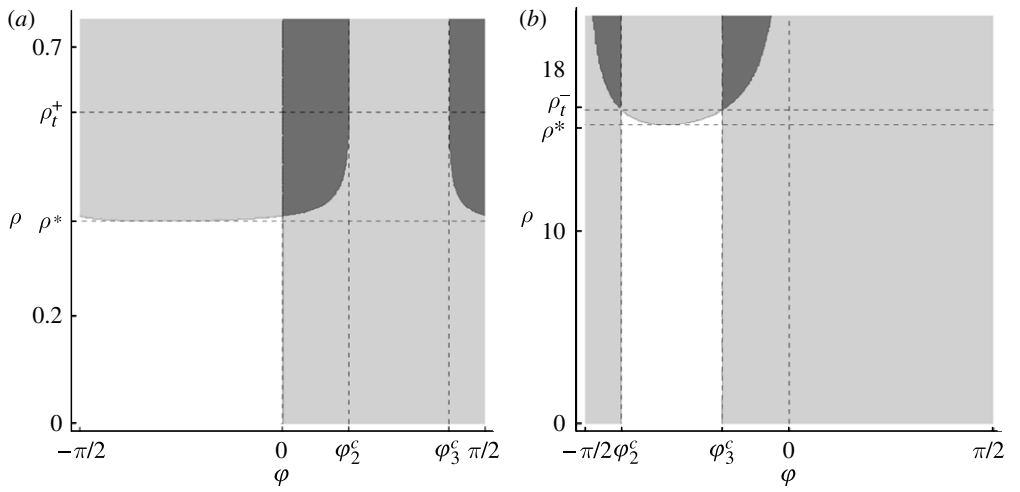

Figure 3. Stability regions as functions of the torsional stiffness ρ and the initial curvature ratio $\tan(\varphi) = \eta = H_x/H_y$: (*a*) $\nu > 0$ and (*b*) $\nu < 0$. Dark grey, light grey and white denote tristability, bistability and monostability, respectively.

(iv) *Material parameters to enhance tristability*

Varying the constitutive parameters β and ν does not change the stability diagrams of figure 3 qualitatively, but influences the size of the tristability regions. The latter are controlled by the values of ρ^*, $\rho_t^{\pm}$ and $\eta_{1,2,3}^c$ given by equations (4.25), (4.26) and (4.16). We focus on the case $\nu > 0$. Provided that ρ is large enough to prevent twisting instabilities, i.e. $\rho > \rho_t^+$, the width of the tristability regions depends only on $\Delta\varphi = \varphi_3^c - \varphi_2^c$; the smaller the $\Delta\varphi$, the larger is the percentage area of the tristability regions in the H_x–H_y plane (figure 3*a*). Figure 4 reports this percentage area of tristability as a function of β and ν, as calculated from (4.16). It increases for β close to ν^2. In the limit case $\beta = \nu^2$, the shell bending stiffness $\bar{\boldsymbol{D}}$ of equation (2.5) becomes singular. Specifically, two eigenvalues vanish: the torsional rigidity and the bending stiffness for curvatures along the direction $\boldsymbol{K} = \{-\nu, 1, 0\}$. It is relevant to note that, when approaching this degeneracy condition, the threshold values of the shear stiffness required to prevent twisting instabilities are finite for $\nu > 0$, while they diverge for $\nu < 0$, with

$$\lim_{\beta \to \nu^2} \rho_t^+ = \frac{3}{4}\nu, \qquad \lim_{\beta \to \nu^2} \rho^* = \frac{\nu}{2} \qquad \text{and} \qquad \lim_{\beta \to \nu^2} \rho_t^- = \infty. \tag{4.27}$$

When seeking to design shells for which tristability may easily be observed experimentally, one must look for the combinations of material parameters that maximize the size of the tristability regions. In this respect, the most interesting scenario occurs for $\nu > 0$, for which the previous analysis concludes with the following two key requirements:

(i) the ratio of the Young's moduli β and the Poisson modulus ν should be as close as possible to the singularity condition $\beta = \nu^2$ and
(ii) the shear stiffness ρ should be larger than the threshold value ρ_t^+ given by equation (4.25), so as to avoid twisting instabilities.

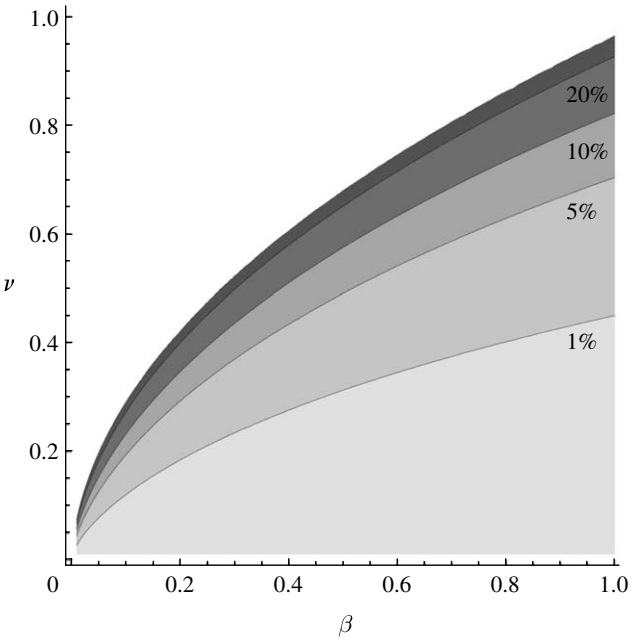

Figure 4. Percentage area of tristability regions in the H_x–H_y plane as a function of the constitutive parameters β and $\nu > 0$. The shear stiffness is assumed sufficiently high ($\rho \geq \rho_t$) to prevent twisting instabilities.

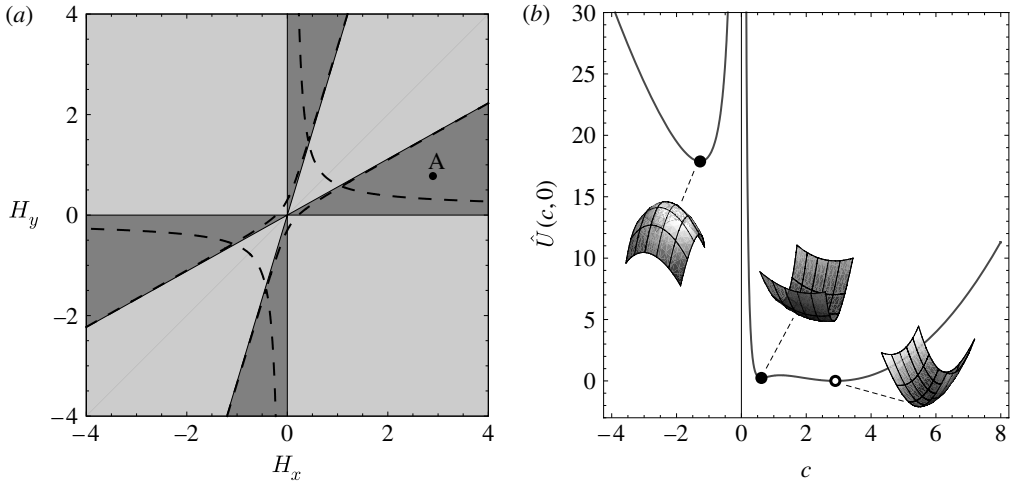

Figure 5. (*a*) Phase diagram for the inextensible model ($\beta = 0.54$, $\nu = 0.7$ and $\rho = 1$). Dark and light grey denote tristabilility and bistability, respectively. The superposed dashed curves represent the stability boundaries calculated with the extensible model for $\phi = 10$. (*b*) The energy $\hat{U}(c, 0)$ for the initial curvature corresponding to point A. The stable equilibria are marked by black points; the white point distinguishes the natural state.

As a representative example of shells with a large tristability range, figure 5*a* reports the phase diagram in the initial curvature space for $\beta = 0.54$, $\nu = 0.7$ and $\rho = 1 > \rho_t^+$, where $\beta \simeq \nu^2 = 0.49$. The lines $H_y = \eta^c_{1,2,3} H_x$ partition the H_x–H_y plane into bistability and tristability regions. To assess the pertinence of the inextensibility assumption, the stability boundaries calculated numerically with the extensible model as for figure 1 are superposed as dashed curves. This confirms that the extensible model behaves asymptotically in the same way as the inextensible one for large curvatures, the stability properties are affected by extensibility only in the neighbourhood of the origin. The comparison with figure 1 also proves the effectiveness of the criteria obtained using the inextensible model in enlarging the tristability regions. Figure 5*b* plots the energy of the inextensible model $\hat{U}(c, 0)$ for the initial curvature corresponding to point A of figure 5*a*; the shell shapes at the three stable equilibria are shown. As noted in the comments on figure 1, there is a second equilibrium separated by a small energy gap from the natural state. The third equilibrium, with c of opposite sign, is at a notably larger energy level.

5. Concluding remarks

This paper has reported on the influence of the material and geometrical properties on the multistable behaviour of uniformly curved thin orthotropic shallow shells. The analysis of the extensible and inextensible shell models provided complementary results. The extensible model showed essential information in the low-curvature regime, revealing the threshold values for the initial curvatures under which the shell is monostable. As a drawback, it called for a numerical analysis to be performed for specific material properties. The numerical investigation, worked out at the same material parameters used by Seffen (2007), disclosed cases of tristability, a novel result. Tristability was suspected by Seffen, but in his exploration he was unable to exhibit more than two stable equilibria. The inextensible model enlightened the asymptotic stability properties in the high curvature limit, the comparison length being the shell thickness. By focusing on untwisted shells, this simplified approach allowed us to solve analytically the dependence of the multistability properties on the material parameters. We conclude that the range of initial curvature leading to tristability may be enlarged by conceiving shells, where the Young's moduli ratio β and the Poisson ratio ν approach the degeneracy condition $\beta = \nu^2$, provided that the shear modulus ρ is large enough to prevent twisting instabilities.

The modelling approach we adopted underpinned the key multistability properties of uniformly curved shells at a cost of several simplifying assumptions. The strongest of these is the uniform curvature hypothesis, which is crucial to obtain analytical results. This hypothesis means neglecting any boundary-layer effect, and concentrating on an averaged interior problem. This is commonly accepted for shells that are free at the boundary and for loadings appearing in the form of uniform initial distortions. In particular, this may include hygrothermal loadings or the actions of active materials, such as piezoelectric fibre composites and shape memory alloys. The uniform curvature model and the results reported here lose their validity for shells with different boundary or loading conditions, such as partially clamped shells and concentrated forces. A point that merits

further attention is a precise assessment of the influence on the stability properties of the coupling between the bending and extensional deformations shown by asymmetric laminates, a contribution that has been omitted in the energy expression (2.4) of the extensible model. We expect the asymptotic results obtained with the inextensible model to remain valid, albeit with a smaller order of accuracy.

This work is intended to provide essential groundwork for the design of variable geometry structures, where small actively controlled deformations may cause major shape changes by exploiting nonlinear phenomena. To meet the requirements of technological applications, directions for future research should encompass the optimization of the lay-ups of multilayered composites leading to the desired constitutive properties of the shell, as well as the definition of control laws suitable to exploit the multistable behaviour. As the control parameters are the components of the imposed curvature, stacking sequences of multiple layers of unidirectional piezoelectric fibre composites and shape memory alloys would provide an effective technological means to control the initial curvature in two orthogonal directions. In this regard, a future extension of this work is to study how the multiparameter piezoelectric actuation techniques presented in Maurini *et al.* (2007) for buckled bistable beams may be adapted to two-dimensional structures.

This work was partially supported by the joint research project PAI Galileo project no. 14383QD, between Université Pierre et Marie Curie—Paris 6 and Università di Roma La Sapienza, and by a programme for cultural and scientific cooperation of Università di Roma La Sapienza, which are gratefully acknowledged.

References

Bowen, C., Butler, R., Jervis, R., Kim, H. & Salo, A. 2007 Morphing and shape control using unsymmetrical composites. *J. Intel. Mater. Syst. Struct.* **18**, 89–98. (doi:10.1177/1045389X07064459)

Calladine, C. 1983 *Theory of shell structures*. Cambridge, UK: Cambridge University Press.

Forterre, Y., Skotheim, J. M., Dumais, J. & Mahadevan, L. 2005 How the venus flytrap snaps. *Nature* **433**, 421–425. (doi:10.1038/nature03185)

Guest, S. & Pellegrino, S. 2006 Analytical models for bistable cylindrical shells. *Proc. R. Soc. A* **462**, 839–854. (doi:10.1098/rspa.2005.1598)

Hyer, M. W. 1981 Calculation of the room-temperature shapes of unsymmetric laminates. *J. Compos. Mater.* **15**, 296–310. (doi:10.1177/002199838101500207)

Kebadze, E., Guest, S. & Pellegrino, S. 2004 Bistable prestressed shell structures. *Int. J. Solids Struct.* **41**, 2801–2820. (doi:10.1016/j.ijsolstr.2004.01.028)

Love, A. E. H. 1906 *A treatise on the mathematical theory of elasticity*. Cambridge, UK: Cambridge University Press.

Mansfield, E. H. 1962 Bending, buckling and curling of a heated thin plate. *Proc. R. Soc. A* **268**, 316–327. (doi:10.1098/rspa.1962.0143)

Mansfield, E. H. 1989 *The bending and stretching of plates*. Cambridge, UK: Cambridge University Press.

Mattioni, F., Weaver, P., Potter, K. & Friswell, M. 2007 Analysis of thermally induced multistable composites. *Int. J. Solids Struct.* **45**, 657–675. (doi:10.1016/j.ijsolstr.2007.08.031)

Maurini, C., Pouget, J. & Vidoli, S. 2007 Distributed piezoelectric actuation of a bistable buckled beam. *Eur. J. Mech. A/Solids* **26**, 837–853. (doi:10.1016/j.euromechsol.2007.02.001)

Norman, A. D., Seffen, K. A. & Guest, S. D. 2008 Multistable corrugated shells. *Proc. R. Soc. A* **464**, 1653–1672. (doi:10.1098/rspa.2007.0216)

Podio Guidugli, P. 1991 *Lezioni sulla Teoria Lineare dei Gusci Elastici Sottili*. Milano, Italy: Masson.

Portela, P., Camanho, P., Weaver, P. & Bond, I. 2008 Analysis of morphing, multi stable structures actuated by piezoelectric patches. *Comput. Struct.* **86**, 347–356. (doi:10.1016/j.compstruc.2007.01.032)

Schultz, M. R., Hyer, M. W., Williams, R. B., Wilkie, W. K. & Inman, D. J. 2006 Snap-through of unsymmetric laminates using piezocomposite actuators. *Compos. Sci. Technol.* **66**, 2442–2448. (doi:10.1016/j.compscitech.2006.01.027)

Seffen, K. A. 2007 'Morphing' bistable orthotropic elliptical shallow shells. *Proc. R. Soc. A* **463**, 67–83. (doi:10.1098/rspa.2006.1750)